Path planning using vehicle slip angle prediction for obstacle avoidance manoeuvres in complex driving scenarios

Kanarachos, S. and Chrysakis, G

Original citation:
Kanarachos, S. and Chrysakis, G. (2016) Path planning using vehicle slip angle prediction for obstacle avoidance manoeuvres in complex driving scenarios. WSEAS Transactions on Systems and Control, volume In press

Path planning using vehicle slip angle prediction for obstacle avoidance manoeuvres in complex driving scenarios

STRATIS KANARACHOS, GEORGIOS CHRYSAKIS
Mechanical, Automotive and Manufacturing Department
Coventry University
3, Gulson Road, Coventry, CV1 2JH
UNITED KINGDOM
stratis.kanarachos@coventry.ac.uk http://www.coventry.ac.uk

Abstract: - When an obstacle suddenly appears in the path of a vehicle a manoeuvre has to be executed to avoid it. In the future, Advanced Driver Assistance Systems will perform this task automatically. However, the plan and execution in real time of an obstacle avoidance manoeuvre is challenging because it has to not only avoid the obstacles but also fulfil additional requirements such as to remain within the road boundaries, satisfy acceleration and jerk limits, avoid excessive vehicle slip angles and respect actuators' limitations. Most of the approaches proposed up to now relax the problem by considering only simple driving scenarios, such as lane change manoeuvres, and thus can't handle complex driving situations. Furthermore, no consideration of the vehicle's slip angle is being taken leading to paths that either cause instability or limit conservatively the maximum yaw rate. In this paper, for the first time, an obstacle avoidance manoeuvre planning method that includes a prediction of the vehicle's slip angle is proposed. The methodology which is based on a finite element method can handle complex driving scenarios and enables the planning of paths that respect vehicle dynamics' limitations. Numerical simulations using a linear bicycle model show the performance of the proposed method and its advantages compared to standard path planning methods.

Key-Words: - obstacle avoidance manoeuvres, path planning, vehicle slip angle prediction

1 Introduction

Today, the main cause of car crashes is human errors in judgment and decision making. The requirement to install, as of 2014 in Europe, an Autonomous Emergency Braking (AEB) System for every new vehicle type will reduce the total number of fatalities and serious injuries in accidents that occur at low speeds. However, in order to improve road safety at high speeds, e.g. above 60 km/h, a new generation of Advanced Driver Assistance Systems (ADAS) capable of planning and controlling the lateral motion of a vehicle is needed. This paper is focusing on this category and in particular on planning obstacle avoidance (OA) maneuvers of ground vehicles at high speeds.

An obstacle avoidance manoeuvre planner essentially consists of a path planner and a lower level path tracking controller that utilizes one or more of the vehicle's actuators e.g. steering wheel and brakes. Different approaches have been already researched and in the following a short review of the main recent contributions is given.

Gray et al investigated the performance of a point mass path planner and concluded that the trajectory generated, although real-time capable, was not always feasible [1]. The lower level tracking controller could not follow the planned path and obstacle collisions were observed in conditions where the obstacle could have been avoided. Thus, they proposed a path planner based on motion primitives which respect a priori the vehicle dynamics constraints. The main drawback is that motion primitives aren't suitable for complex driving scenarios where arbitrary boundary conditions may hold.

Shim et al investigated a path planning method which utilizes sixth order polynomials [2]. The polynomials' unknown coefficients are computed a) by determining the position, velocity and acceleration at the beginning and end of the trajectory and b) by solving in real time a minimization problem that minimizes the travel distance. A semi-analytical expression has been derived for the case of zero initial and desired lateral velocities and accelerations. The performance of the path planner in combination with a model predictive path tracking controller was evaluated in a simulation environment. One of the disadvantages

of higher order polynomials is that they can generate oscillatory paths.

Isermann et al. utilized a sigmoid function to model the manoeuvres by observing that obstacle avoidance paths form an "S" shape in straight road segments [3]. The sigmoidal is parameterized using three parameters which are calculated by solving a system of nonlinear algebraic equations. The solution gives an evasive path with minimal length which respects different system limits such as maximum lateral acceleration, maximal jerk and dynamics of the steering actuator. The method has been evaluated both experimentally and computationally. Disadvantage of the method is that it has been developed for straight paths only.

A methodology suited for planning obstacle avoidance manoeuvres for general driving situations has been presented in [4] and [5]. The first contribution deals with nonlinear manoeuvres where the tire operates in the nonlinear region, while the latter with highly nonlinear manoeuvres that also cause tire saturation. Both methods are based on Pontryagin's Maximum Principle and reformulate the obstacle avoidance problem into a direct optimization problem with only a few parameters. However, they have a high computational burden. To circumvent it an efficient iterative solution method based on finite elements has been proposed in [6]. A disadvantage of this method is that the path planner considered conservative yaw rate limits.

The present contribution, for the first time to our knowledge, predicts the evolution of vehicle's slip angle for a planned obstacle avoidance manoeuvre and integrates the prediction to the path planning methodology. Furthermore, it calculates based on the inverse dynamics principle the required steering input to execute the manoeuvre. The performance of the proposed method is evaluated and compared to other path planning methods in a simulation environment.

The rest of the paper is organized as follows. In Sections 2 a short overview of the vehicle model used and the finite element concept are given. In section 3 the method developed to predict vehicle's slip angle is presented. In Section 4 the obstacle avoidance planner is evaluated and compared with another known method for different driving scenarios. In section 5 the sensitivity of the proposed method is evaluated for tire model uncertainties. The analysis and evaluation is performed in Matlab simulation environments. In Section 6 conclusions and future research directions are drawn.

2 Mathematical model

2.1 Vehicle model

The proposed method is based on the hypothesis that it is difficult to obtain and use in real-time a very detailed vehicle model. In this context, a model that can capture the gross vehicle motion is employed. Furthermore, it is assumed that the vehicle is equipped with an Electronic Stability Control (ESC) system, such as the one described in [7]. The ESC and path tracking system utilize the same yaw rate limit. Any command above the yaw rate threshold will cause ESC's system activation and thus bring the vehicle from a path tracking to a stability mode.

The two track vehicle model (TTVM), shown in Figure 1, is used to derive the equations of motion described by forward velocity u_f, lateral velocity v and yaw rate r (Pacejka, 2005) [8].

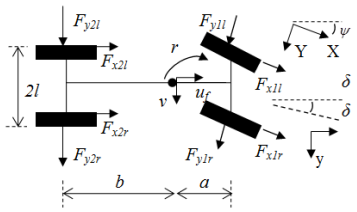

Figure 1. Top view (left) and front view (right) of TTVM

For simplification reasons shock absorbers and suspension springs are neglected. Also neglected are roll angle, steer angle and roll axis inclination which are assumed small enough. Effects of additional steer angles due to suspension kinematics and steer compliance are ignored [8]. The equations of motion, Eq. (1)-(3), are:

$$m \cdot \left(\dot{u}_f - r \cdot v\right) = \sum F_x = F_{x1} + F_{x2} \quad (1)$$

$$m \cdot \left(\dot{v} + r \cdot u_f\right) = \sum F_y = F_{y1} + F_{y2} \quad (2)$$

$$I_z \cdot \dot{r} = \sum M = a \cdot F_{y1} - b \cdot F_{y2} \quad (3)$$

where m is the mass, I_z the moment of inertia, a and b the distances from centre of gravity to front and rear axle respectively, $F_{x1}=F_{x1l}+F_{x1r}$ and $F_{x2}=F_{x2l}+F_{x2r}$ are the longitudinal forces on the front and rear axle respectively and $F_{y1}=F_{y1l}+F_{y1r}$ and $F_{y2}=F_{y2l}+F_{y2r}$ are the lateral forces on the front and rear axle respectively and u_f the forward velocity.

Vehicle velocities $\dot{X}$ and $\dot{Y}$ in the global coordinate system $O(X,Y)$ are a function of local

velocities u_f and v expressed in the vehicle coordinate system *o(x,y)* and angle ψ (shown in Figure 1). The transformation from one coordinate system to the other is obtained by:

$$\begin{bmatrix} \dot{X} \\ \dot{Y} \\ \dot{\psi} \end{bmatrix} = \begin{bmatrix} \cos\psi & -\sin\psi & 0 \\ \sin\psi & \cos\psi & 0 \\ 0 & 0 & 1 \end{bmatrix} \cdot \begin{bmatrix} u_f \\ v \\ r \end{bmatrix} \quad (4)$$

The vehicle's trajectory (*X*,*Y*), expressed in the global coordinate system, is:

$$X = \int_0^T \dot{X} \cdot \cos\psi \cdot dt \quad (5)$$

$$Y = \int_0^T \dot{Y} \cdot \sin\psi \cdot dt \quad (6)$$

where *T* is the manoeuvring time.

2.2 The finite element method

Planning obstacle avoidance manoeuvres has a high computational burden because we need to optimize in real time the solution of a system of differential equations. Since no reference trajectory, e.g. road lane, is available for such manoeuvres both states and inputs of the system are unknown for the total manoeuvre. A finite element concept, which reduces the computational load significantly, has been proposed. The method recasts the problem from a real time optimization one into a deterministic linear algebraic and thus eases calculations.

A schematic of the approach is shown in Figure 2. The total path is decomposed in *N* finite elements/segments. Each finite element is denoted with a number *n=1…N*, and has two nodes: the start node n_a and end node n_b. The obstacle avoidance path is constructed by joining end node n_b and start node $(n+1)_a$ of two consecutive finite elements *n* and *n+1*, for *n=1:..:N-1*.

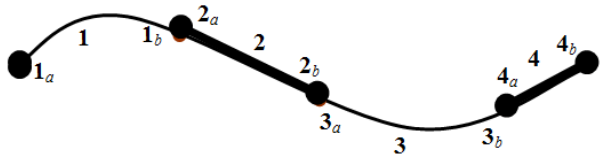

Figure 2. Emergency path decomposed in four finite elements

Each finite element is parameterized using two variables: time span $t_{n,span}$and the highest order constrained state variable. Time span $t_{n,span}$may be uniformly chosen by decomposing the total maneuvering time in *n* segments or by considering other parameters such as change of tire-road friction coefficient μ and road curvature. In this paper, angular jerk is the highest order constrained state variable and assumed constant in each segment, $\dddot{r}_n = a_{3n}$ for $t_n \in [0, t_{n,span}]$. In this context, angular acceleration $\dot{r}_n$, velocity r_n and position θ_n are:

$$\dddot{r}_n = a_{3n} \quad (7)$$

$$\dot{r}_n = \int_0^{t_{n,span}} \dddot{r}_n \cdot dt = a_{3n} \cdot t + a_{2n} \quad (8)$$

$$r_n = \int_0^{t_{n,span}} \dot{r}_n \cdot dt = 0.5 \cdot a_{3n} \cdot t^2 + a_{2n} \cdot t + a_{1n} \quad (9)$$

$$\theta_n = \int_0^{t_{n,span}} r_n \cdot dt = \frac{1}{6} \cdot a_{3n} \cdot t^3 + 0.5 \cdot a_{2n} \cdot t^2 + a_{1n} \cdot t + a_{0n} \quad (10)$$

where $t_n \in [0, t_{n,span}]$.

The states $y_n = \begin{bmatrix} \dot{r}_{n,a} & r_{n,a} & \theta_{n,a} & \dot{r}_{n,b} & r_{n,b} & \theta_{n,b} \end{bmatrix}^T$ at the boundaries of the finite element are expressed in matrix form as:

$$\mathbf{y_n} = \mathbf{A_n} \cdot \mathbf{x_n} \quad (11)$$

$$\mathbf{y_n} = \begin{bmatrix} \dot{r}_{n,a} & r_{n,a} & \theta_{n,a} & \dot{r}_{n,b} & r_{n,b} & \theta_{n,b} \end{bmatrix}^T \quad (12)$$

$$\mathbf{x_n} = \begin{bmatrix} a_{3n} & a_{2n} & a_{1n} & a_{0n} \end{bmatrix}^T \quad (13)$$

$$\mathbf{A}_n = \begin{bmatrix} 0 & 1 & 0 & 0 \\ 0 & 0 & 1 & 0 \\ 0 & 0 & 0 & 1 \\ t_{nspan} & 1 & 0 & 0 \\ 0.5 \cdot t_{nspan}^2 & t_{nspan} & 1 & 0 \\ 0.1667 \cdot t_{nspan}^3 & 0.5 \cdot t_{nspan}^2 & t_{nspan} & 1 \end{bmatrix} \quad (14)$$

The finite element matrix $\boldsymbol{A}_n$ constitutes the basis for joining subsequent elements and deriving the system's solution. For a detailed description the reader is referred to [6].

3 Obstacle manoeuvre planning

3.1 Vehicle slip angle β prediction

Most of the algorithms neglect the evolution of vehicle's slip angle β for the planned path or employ –as countermeasure- conservative limits for yaw rate r. In this paper, a different strategy is followed; the coupled equations of motion are solved iteratively to predict the evolution of slip angle β and include it in the planning algorithm.

Yaw rate r is parameterized in each finite element as a second order polynomial. In the same context and in order to satisfy the linearized equations of motion (2)-(3) lateral velocity v is also modelled as a second order polynomial:

$$v = b_{2n} \cdot t^2 + b_{1n} \cdot t + b_{0n} \quad (15)$$

The main assumption taken, for the linearization of Equations (2) and (3), is that the tire lateral force is a linear function of the slip angle, thus $F_{y1} = C_1 \cdot a_1$ and $F_{y2} = C_2 \cdot a_2$. The symbols C_1 and C_2 denote the cornering stiffness of the front and rear tires and a_1 and a_2 the slip angles of the front and rear tires respectively. According to Lee et al (2014) this is a valid assumption since the obstacle avoidance manoeuvre planner is activated at velocities higher than 60 *km/h* and in general, when a driver drives a vehicle along the road with velocity higher than 60 *km/h*, the tire slip angle is maintained under 5° [16]. The tire stiffness's C_1 and C_2 are defined in an averaged sense, as described in Snider (2009) [9]. The usage of linear constrained vehicle models has been proved more effective than that of nonlinear ones [17].

The coefficients b_{2n}, b_{1n} and b_{0n} are computed using the following iterative formula:

$$b_{2n,i+1} = \begin{bmatrix} \frac{(a^2 \cdot C_1 + b^2 \cdot C_2) \cdot a_{sn}}{2 \cdot a^2 \cdot (C_1 + C_2)} \\ + \frac{2 \cdot a \cdot (a \cdot C_1 - b \cdot C_2) \cdot b_{2n,i}}{2 \cdot a^2 \cdot (C_1 + C_2)} \end{bmatrix} \quad (16)$$

$$b_{1,i+1} = \frac{1}{C_1 + C_2} \cdot \begin{bmatrix} -2 \cdot m \cdot b_{2n,i+1} \cdot u_f \\ + \frac{I \cdot a_{sn} \cdot u_f}{a^2} \\ + \frac{(a^2 \cdot C_1 + b^2 \cdot C_2) \cdot a_{2n}}{a^2} \\ + \frac{a \cdot (a \cdot C_1 - b \cdot C_2) \cdot b_{1n,i}}{a^2} \end{bmatrix} \quad (17)$$

$$b_{0,i+1} = \frac{1}{C_1 + C_2} \cdot \begin{bmatrix} -m \cdot b_{1n,i+1} \cdot u_f \\ + \frac{I \cdot a_{2n} \cdot u_f}{a^2} \\ + \frac{(a^2 \cdot C_1 + b^2 \cdot C_2) \cdot a_{1n}}{a^2} \\ + \frac{a \cdot (a \cdot C_1 - b \cdot C_2) \cdot b_{0n,i}}{a^2} \end{bmatrix} \quad (18)$$

where i is the iteration number. The solution converges after 3-4 iterations. The advantage of representing the slip angle with a second order polynomial is the straightforward calculation of its maximum and minimum values within each finite element. The derivation of the formulas listed in Equations (16)-(18) is lengthy and is subject of another paper currently under preparation.

3.2 Path planning using vehicle slip angle β prediction

The lateral acceleration at the centre of gravity of the vehicle is given by:

$$a_y = u_f \cdot r + \dot{v} \quad (19)$$

Since,

$$v = u_f \cdot tan\beta \quad (20)$$

the lateral acceleration can be related to the yaw rate r and the vehicle slip angle β by the equation:

$$a_y = u_f \cdot r + tan\beta \cdot \dot{u}_f + \frac{u_f \cdot \beta}{\sqrt{1+tan^2\beta}} \quad (21)$$

Lateral acceleration a_y must be bounded by the tire-road friction coefficient μ as follows:

$$a_y \leq \mu \cdot g \quad (22)$$

Equation (22) is usually the dominant constraint when planning time optimal obstacle avoidance paths. The first term in the calculation of lateral acceleration in Equation (21) is the most important. Since the evolution of slip angle β is unknown most algorithms either neglect the second and third term or substitute it with a conservative constant value e.g. $tan\beta \cdot \dot{u}_f + \frac{u_f \cdot \beta}{\sqrt{1+tan^2\beta}} = 0.15 \cdot \mu \cdot g$. In this contribution, since a prediction of vehicle slip angle β is performed, all terms are considered. Last but not least, depending on driver's capabilities, a maximum slip angle limit is set [10], e.g.:

$$\beta \leq \beta_{lim} \quad (22)$$

The threshold β_{lim} is identified either experimentally or computationally by performing aggressive manoeuvres and evaluating the prediction accuracy of the linearized model.

3.3 Steering input δ computation

Integrated vehicle controllers (Alirezaei, 2013) optimally combine the brakes, steering wheel and suspension actuators of a vehicle and thus achieve optimal (momentarily) feedback performance [11]. However, it seems that the inherently slower dynamics of the steering system -compared to the braking system- restricts its overall contribution in dynamic manoeuvres. This is in contrast with the already known significant advantages that active steering offers in vehicles dynamics [12]. Furthermore, in many future vehicles -due to cost, complexity, reliability and other reasons- the subsystems won't be utilized concurrently for the same objective. This paper is based on the assumption that an active steering system is utilized as an open loop controller (guidance part), while an Electronic Stability Control system is responsible for the vehicle's closed loop stability.

In this case, and since the yaw rate r and vehicle slip angle β are known the steering input δ is calculated based on the inverse dynamics principle and given by formula (23).

A schematic of the proposed obstacle avoidance algorithm is shown in Figure (3). The manoeuvring period is selected based on a threat assessment criterion like time to steer [13]. N_c is the total number of constraints and N_u is the total number of unknowns.

$$\delta = \frac{1}{a \cdot C_1} \cdot \left[\begin{array}{l} \left(\frac{(a^2 \cdot C_1 + b^2 \cdot C_2) \cdot a_{3n}}{2 \cdot u_f \cdot a} + \frac{2 \cdot a \cdot (a \cdot C_1 - b \cdot C_2) \cdot b_{2n}}{2 \cdot u_f \cdot a} \right) \cdot t^2 \\ + \left(\frac{\frac{I \cdot a_{3n} \cdot u_f}{u_f \cdot a}}{+ \frac{(a^2 \cdot C_1 + b^2 \cdot C_2) \cdot a_{2n}}{u_f \cdot a}} + \frac{a \cdot (a \cdot C_1 - b \cdot C_2) \cdot b_{1n}}{u_f \cdot a} \right) \cdot t \\ + \left(\frac{\frac{I \cdot a_{2n} \cdot u_f}{u_f \cdot a}}{+ \frac{(a^2 \cdot C_1 + b^2 \cdot C_2) \cdot a_{1n}}{u_f \cdot a}} + \frac{a \cdot (a \cdot C_1 - b \cdot C_2) \cdot b_{0n}}{u_f \cdot a} \right) \end{array} \right] \quad (23)$$

The inherent limitations of the TTVM model apply to the proposed method. It will not approximate vehicle motion well at very low speeds, during tight manoeuvres or during high speed manoeuvring where the influence of suspension geometry is critical. It is also known from Mitschke (2004) that the linear bicycle model is valid only when $F_{y\max} < \frac{1}{3} \cdot \mu \cdot F_z$, effectively for lateral accelerations up to 0.4 g's for dry road conditions and 0.05 g's on icy condition [14].

4 Numerical simulations

The proposed method has been tested for an extensive number of driving scenarios in Matlab's

simulation environment. The numerical examples are based on the vehicle data and tire parameters listed in Table 1. In the following the numerical results for two driving scenarios, that illustrate the features of the proposed algorithm, are presented and discussed.

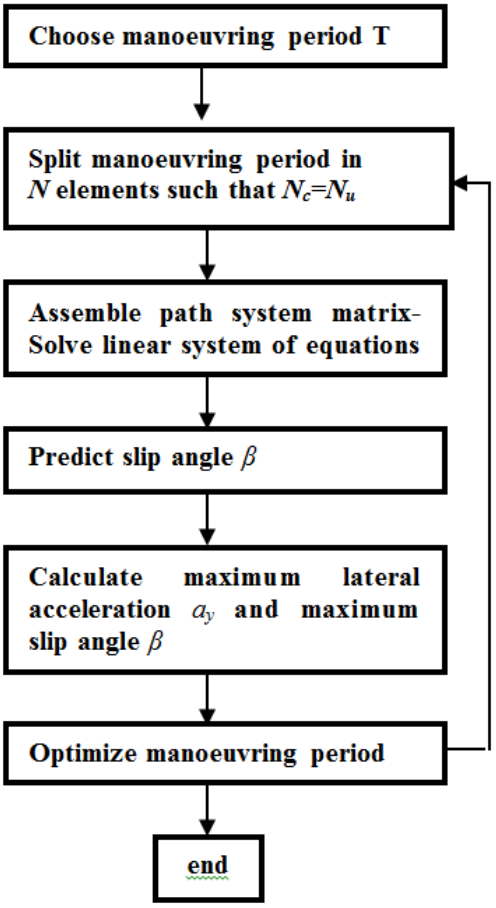

Figure 3. Obstacle avoidance planning algorithm

Table 1 Vehicle parameters.

Name	Parameter	Value
Vehicle mass	m [kg]	870
Distance from ground to CG	h [m]	0.58
Moment of inertia - to z axis	I_z [kgm^2]	1440
Half length of the wheel axle	l [m]	0.765
Distance of front axle from cog	a [m]	1.2
Distance of rear axle from cog	b [m]	0.90
Cornering stiffness front tires	C_1 [N/rad]	23000
Cornering stiffness rear tires	C_2 [N/rad]	19000

4.1 Driving scenario 1: Obstacle avoidance manoeuvre – straight path, TTC=2.5 s

In the first driving scenario the vehicle is moving at a speed u_f=30 m/s, when suddenly an obstacle appears in its path. The road segment is straight and the vehicle has to perform a lane change to avoid it (see Figure 4). The time to collision (TTC) is T=2.5s. To avoid the collision the vehicle has to displace laterally by $Y_{des} = 3\,m$. The tire-road friction coefficient is assumed to be equal to μ=1. The obstacle avoidance manoeuvre is decomposed in four finite elements of equal time T_n=0.625 s. The manoeuvring time wasn't optimized (last step in obstacle avoidance algorithm, Figure 3).

The numerical results obtained are shown in Figures 5-9. The abbreviation ODE stands for Ordinary Differential Equations while FE for Finite Element. From the results it is evident that the yaw rate calculation in the finite element method and the ODE solution match quite well. The correlation coefficient between the ODE and FE solution for the yaw angle r is R=0.995, while for the slip angle β is R=0.86. The maximum slip angle in the FE method is higher than the maximum one predicted by the ODE solution. It is highlighted that the ratio $\beta_{maxFE}/\beta_{maxODE}$=1.42. Furthermore, the FE solution has a phase lead of about 0.1 s with respect to the ODE solution. This means that the FE solution is on the conservative side.

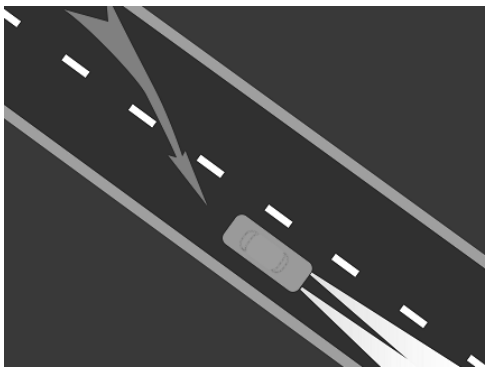

Figure 4. Obstacle avoidance manoeuvre

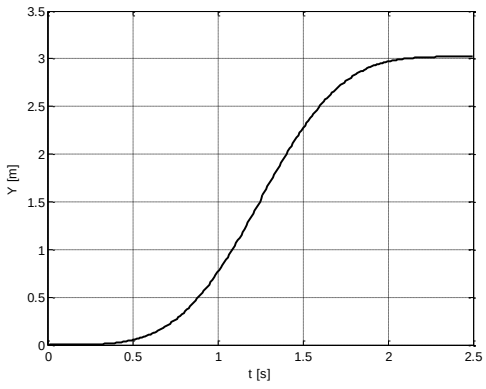

Figure 5. Lateral displacement Y versus time for driving scenario 1

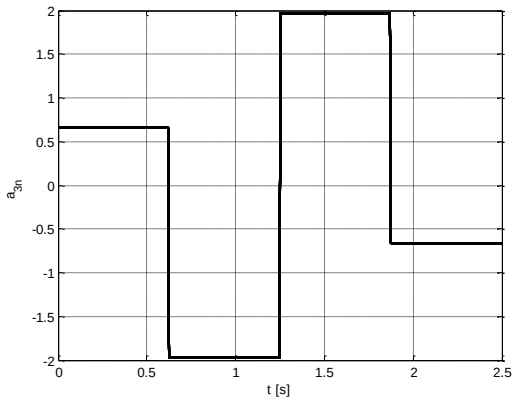

Figure 6. Angular jerk a_{3n} versus time for driving scenario 1

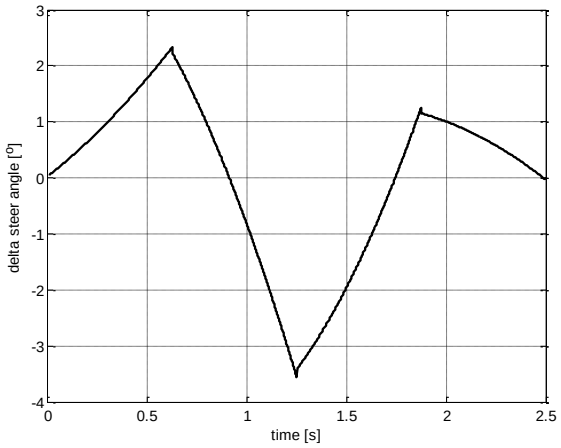

Figure 7. Steering input δ versus time for driving scenario 1

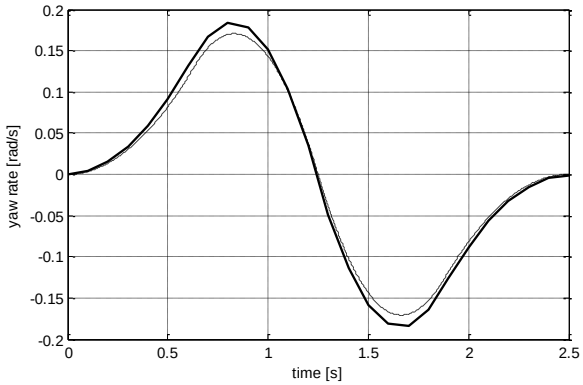

Figure 8. Yaw rate r versus time for driving scenario 1(solid line: ODE solution, dashed line: FE solution)

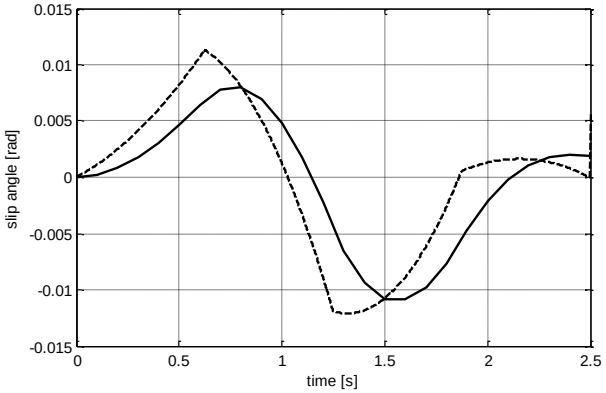

Figure 9. Slip angle β versus time for driving scenario 1 (solid line: ODE solution, dashed line: FE solution)

4.2 Driving scenario 2: Obstacle avoidance manoeuvre – straight path, TTC=1.8 s

In the second driving scenario the vehicle is travelling again at a speed u_f=30 m/s, when suddenly an obstacle appears in its path. The road segment is straight and the vehicle has to perform a lane change to avoid it (see Figure 4). In this case, TTC is T=1.8s and to avoid the collision the vehicle has to displace laterally by $Y_{des} = 3\,m$. As a result the vehicle has to operate in the highly nonlinear region. As in driving scenario 1, the tire-road friction coefficient is assumed to be equal to μ=1, the obstacle avoidance manoeuvre is decomposed in four finite elements of equal time T_n=0.625 s and the manoeuvring time wasn't optimized.

The numerical results obtained for driving scenario 2 are shown in Figures 10-14. From the results it is evident that the yaw rate calculation in the finite element method and the ODE solution match quite well. The correlation coefficient between the ODE and FE solution for the yaw angle r is R=0.992, while for the slip angle β is R=0.74. The maximum slip angle predicted by the FE method is β_{maxFE}=1.48^o while by the ODE is β_{maxODE}=0.97^o. The FE solution has a phase lead of about 0.1s. This means that the FE calculation is conservative.

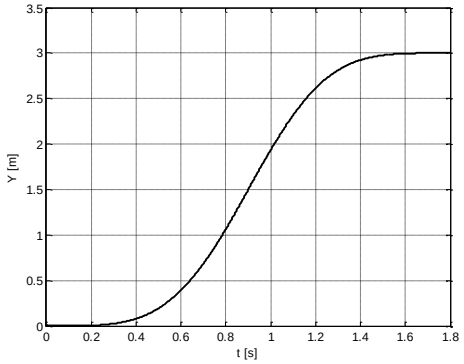

Figure 10. Lateral displacement Y versus time for driving scenario 2

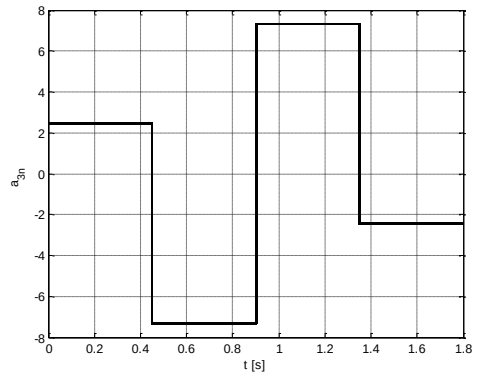

Figure 11. Angular jerk a_{3n} versus time for driving scenario 2

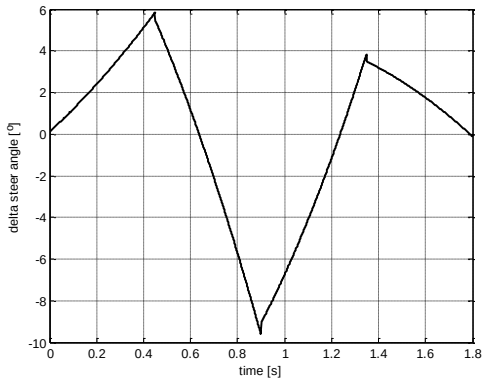

Figure 12. Steering input δ versus time for driving scenario 2

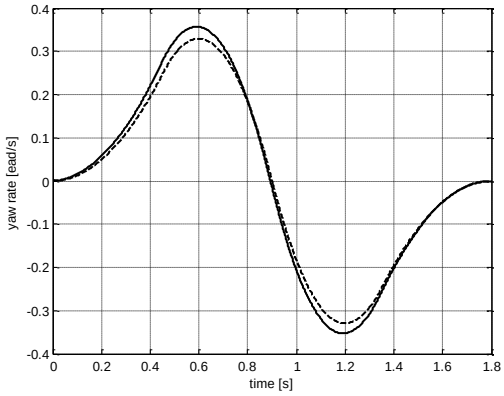

Figure 13. Yaw rate r versus time for driving scenario 2 (solid line: ODE solution, dashed line: FE solution)

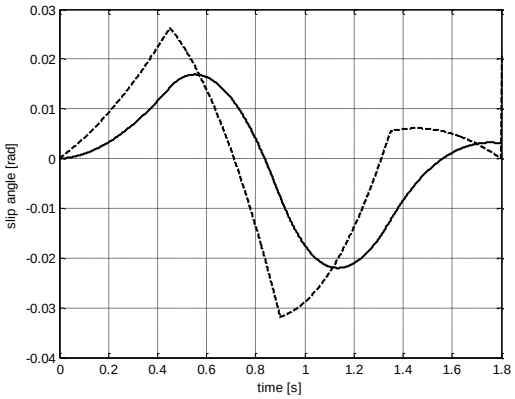

Figure 14. Slip angle β versus time for driving scenario 2 (solid line: ODE solution, dashed line: FE solution)

From the numerical examples it becomes clear that the vehicle yaw rate r is predicted accurately by the FE solution with a correlation coefficient R>0.992. Furthermore, the steering input δ generates indeed the desired obstacle avoidance trajectory. However, the discrepancy between the ODE and FE solutions is larger for the slip angle β. Nevertheless, the correlation between the two solutions - for highly dynamic manoeuvres - is quite high in the range of R=0.75-0.85. Furthermore, the phase lead as well as the ratio $\beta_{maxFE}/\beta_{maxODE}$ is almost constant and independent of the manoeuver type, which means that it can be compensated for. Differently, in order to increase the accuracy of the slip angle β prediction using the FE method a finer discretization of the manoeuvring period T, by utilizing more finite elements is required.

5 Sensitivity analysis

The sensitivity of yaw rate r and vehicle slip angle β with respect to the different model parameters ad especially the tire cornering stiffness's C_1 has to be considered early in the design phase [15]. Thus, the sensitivity of the method has been studied extensively and presented for the two aforementioned driving scenarios. In particular we have studied the variation of steering angle δ in case the front tire cornering stiffness is in the range $[0.85\cdot C_1, 1.15\cdot C_1]$. The results for the two driving scenarios are shown in Figures 15 & 16. It is evident that the steering angle varies in a narrow range, usually below 0.3^o. This essentially means that a closed loop control system could easily reject the disturbances caused by tire model uncertainties.

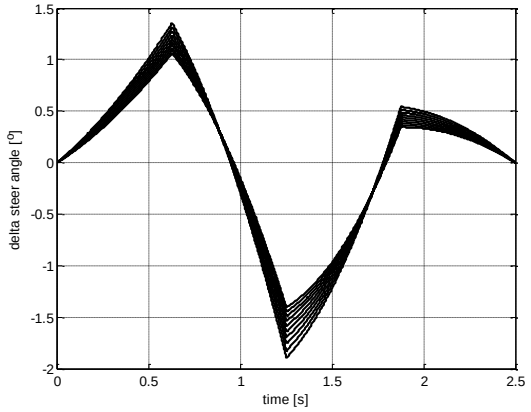

Figure 15. Steering angle δ variation versus time for a range of front tire cornering stiffness's – Driving scenario 1

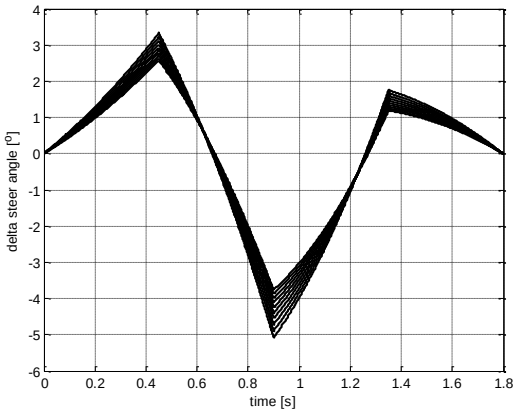

Figure 16. Steering angle δ variation versus time for a range of front tire cornering stiffness's – Driving scenario 2

6 Conclusions – Future research directions

In this paper, for the first time, a methodology for planning obstacle avoidance manoeuvers by considering also the slip angle evolution has been presented. In most obstacle avoidance algorithms the influence of slip angle β is either neglected or conservatively considered. In the first case paths that cause excessive vehicle slip angles are planned, while in the second the maximum yaw rate is unnecessarily constrained.

The proposed methodology is based on the finite element concept. A uniform time grid is used to discretize the manoeuvring period T. The number of finite elements depends on the number of desired states and in the simplest case of a boundary value problem is equal to four. In each finite element the angular jerk $\dddot{r}_n$ is considered constant and assuming this the yaw rate r, orientation θ, lateral displacement Y and vehicle slip angle β are computed. The proposed formulation leads to an algebraic system which can be easily solved. The advantage of the proposed method is the low computational burden in computing the maximum values of yaw rate r and slip angle β which are required for computing time optimal paths.

The yaw rate evolution r is predicted very accurately using the FE method. The correlation between the FE and ODE solution is greater than R>0.992. Furthermore, the steering angle input δ is accurately computed generating indeed the desired trajectories. A sensitivity analysis has shown that the solution is relatively insensitive to the assumed tire cornering stiffness. The slip angle β prediction is less good compared to the yaw rate. The correlation between FE and ODE solutions is greater than R>0.74, which is high but considerably less than the one achieved for the yaw rate. The ratio between the maximum slip angle predicted by the FE and ODE solution is in the range $\beta_{maxFE}/\beta_{maxODE}\approx$1.5. The same ratio holds for different driving scenarios which mean that it can be compensated for. In the future we will study the influence of the finite element influences on the accuracy of the slip angle prediction.

References

1. Gray, A., Yiqi Gao, Lin, T., Hedrick, J.K., Tseng, H.E., Borrelli, F. (2012) 'Predictive control for agile semi-autonomous ground vehicles using motion primitives', *Proceedings of the American Control*

Conference 2012, pp. 4239-4244, 27-29 June 2012.

2. Shim, T., Adireddy G. and Yuan, H. (2012) 'Autonomous vehicle collision avoidance system using path planning and model-predictive-control-based active front steering and wheel torque contro', *Proceedings of the Institution of Mechanical Engineers, Part D: Journal of Automobile Engineering*, Vol. 226, pp. 767-778.
3. Isermann, R., Mannale, R., Schmitt, K. (2012) 'Collision-avoidance systems PRORETA: Situation analysis and intervention control', *Control Engineering Practice*, Vol. 20, No.11, pp. 1236-1246.
4. Kanarachos, S., and Kanarachos, A., (2013) 'Minimum order bang-bang guidance for feedforward obstacle avoidance steering maneuvers of vehicles', *International Journal of Automotive Technology*, Volume 14 (1), pp. 37-46.
5. Kanarachos, S., (2014), 'A new min-max methodology for computing optimised obstacle avoidance steering manoeuvres of ground vehicles', *International Journal of Systems Science*, Vol. 45 (5), pp. 1042-1057.
6. Kanarachos, S. Alirezaei, M., (2015), 'An adaptive finite element method for computing emergency maneuvers of ground vehicles in complex driving scenarios', *International Journal of Vehicle Systems Modeling and Testing*, accepted.
7. Shyrokau, B., Wang, D., Savitski, D. and Ivanov, V., (2013) 'Vehicle dynamics control with energy recuperation based on control allocation for independent wheel motors and brake system', Int. J. Powertrains, vol. 2, No. 2/3, pp. 153-181, 2013
8. Pacejka, B. (2005) 'Tire and Vehicle Dynamics' *Society of Automotive Engineers*, Warrendale
9. Snider, JM. (2009) 'Automatic Steering Methods for Autonomous Automobile Path Tracking', *CMU-RI-TR-09-08 report*, Carnegie Mellon University
10. van Zanten, A., (2002) 'Evolution of electronic control systems for improving the vehicle dynamic behavior', *Proc. Int. Symp. Advanced Vehicle Control (AVEC'02)*, Hiroshima, Japan, Sep. 2002, pp. 7–15.
11. Alirezaei, M.; Kanarachos, S.; Scheepers, B.; Maurice, J.P., (2013) 'Experimental evaluation of optimal Vehicle Dynamic Control based on the State Dependent Riccati Equation technique', *American Control Conference (ACC), 2013* , pp.408-412, 17-19 June 2013
12. Ackermann, J., Buente, T., Odenthal, T., (1990) 'Advantages of active steering for vehicle dynamics control', 29th Conference on Decision and Control, Honolulu, 1990
13. Brännström, M., Coelingh, E. and Sjöberg, J., (2010) 'Model-Based Threat Assessment for Avoiding Arbitrary Vehicle Collisions', *IEEE Transactions on Intelligent Transportation Systems*, Vol. 11 (3), pp. 658-669.
14. Mitschke, M. and Wallentowicz, H. (2004), 'Dynamik der Kraftfahrzeuge', Spinger, 2004
15. Kanarachos, S. (2013) 'Design of an intelligent feed forward controller system for vehicle obstacle avoidance using neural networks', *International Journal of Vehicle Systems Modelling and Testing*, Vol. 8, No.1, pp. 55 – 87.
16. Lee, J., Choi, J., Yi, K., Shin, M., Ko, B., (2014), 'Lane-keeping assistance control algorithm using differential braking to prevent unintended lane departures', *Control Engineering Practice*, Vol. 23, pp. 1-13.
17. Gray, A.; Yiqi Gao; Lin, T.; Hedrick, J.K.; Borrelli, F., (2013) 'Stochastic predictive control for semi-autonomous vehicles with an uncertain driver model', *Intelligent Transportation Systems - (ITSC), 2013 16th International IEEE Conference on* , vol., no., pp.2329,2334, 6-9 Oct. 2013